

Three-Dimensional Paper Microfluidic Devices Assembled Using the Principles of Origami

Hong Liu and Richard M. Crooks*

Department of Chemistry and Biochemistry, Center for Electrochemistry, and Center for Nano- and Molecular Science and Technology, The University of Texas at Austin, 1 University Station, A5300, Austin, Texas 78712-0165, United States

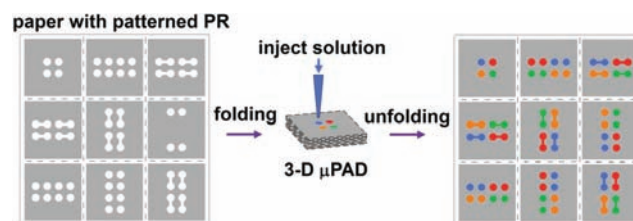
S Supporting Information

ABSTRACT: We report a method, based on the principles of origami (paper folding), for fabricating three-dimensional (3-D) paper microfluidic devices. The entire 3-D device is fabricated on a single sheet of flat paper in a single photolithographic step. It is assembled by simply folding the paper by hand. Following analysis, the device can be unfolded to reveal each layer. The applicability of the device to chemical analysis is demonstrated by colorimetric and fluorescence assays using multilayer microfluidic networks.

Here we report a method for fabricating three-dimensional (3-D) paper microfluidic devices that is based on the principles of origami (paper folding). The concept is illustrated in Scheme 1. Using this method, the entire device is fabricated on a single sheet of flat paper, and then it is assembled by simple paper folding. This method is important for several reasons. First, instead of sequential layer-by-layer fabrication, which is the usual approach for preparing 3-D microfluidic systems,^{1–3} the entire device is fabricated on one piece of paper in a single photolithographic step. This speeds the fabrication process and reduces cost. Second, the multilayer device is assembled by simple paper folding, which can be completed in less than 1 min without tools or special alignment techniques. Third, the device can be easily unfolded so that all layers, rather than just the surface, can be used for parallel analysis. Fourth, incorporation of additional intermediate layers should not result in much additional fabrication overhead.

The principles of 2-D and 3-D microfluidic paper analytical devices (μ PADs) have been described by Whitesides and co-workers,^{3–7} and a number of interesting applications have been reported.^{3,5–12} Briefly, for 2-D μ PADs, microfluidic channels and reservoirs are fabricated by patterning channel walls on chromatography paper using a hydrophobic material, such as photoresist (PR) or wax. Aqueous solutions are then driven along the hydrophilic paper channels by capillary action. For 3-D μ PADs,^{3,13} individual layers are patterned sequentially by photolithography and then stacked using double-sided tape. Holes are punched in the tape using a laser cutter, and the resulting holes are filled with cellulose powders³ or are compressed¹³ to provide vertical connections between adjacent layers. The results of an analysis are determined using colorimetric detection on one of the two surface layers. The 3-D μ PADs show great promise for applications such as power-free, point-of-care detection and diagnosis, particularly in underdeveloped or remote areas. However, as presently practiced, device fabrication requires a photolithographic step for each layer and then laser cutting of vias to establish fluidic

Scheme 1



connections between layers. Moreover, assembly of the device using double-sided tape is irreversible so that only the surface layer can be used for colorimetric detection. The approach we describe addresses these points.

As previously discussed, 3-D μ PADs are fabricated by stacking 2-D layers. An alternative approach is based on the principles of origami. Origami is the traditional Japanese art of paper folding, and it has been in use for \sim 400 years to construct 3-D geometries starting with a single piece of flat paper. Within the context of modern science and engineering, there has not been much interest in origami. However, there is one report in which it was used to fabricate 3-D printed circuit boards in the shapes of airplanes and cranes.¹⁴ With that as a starting point, we show here that origami can be used to fabricate simple and functional microfluidic devices, which we call origami paper analytical devices (*o*PADs), having several highly desirable characteristics.

Figure 1a shows a piece of chromatography paper that has been patterned with channels, reservoirs, and a frame (to provide a template for subsequent folding) fabricated in a single photolithographic step. The fabrication process is based on previously reported procedures³ and is described in the Supporting Information (SI). As reported previously,⁵ the entire photolithographic process can be performed without a cleanroom, using just a hot plate, UV lamp, and a mask produced on a printer. Following photolithography, the 3-D device was assembled by folding the paper along the lithographically defined frame. The frame ensures that the channels and reservoirs are properly aligned after folding into the 3-D assembly. The folding sequence is provided in Figure S1 of the SI. The four corners of the folded paper were trimmed, as shown in parts b and c of Figure 1, to accommodate an aluminum clamp (Figure 1d). Solutions could then be injected into the four holes drilled into the top aluminum plate of the clamp (Figure 1d).

Received: July 31, 2011

Published: October 17, 2011

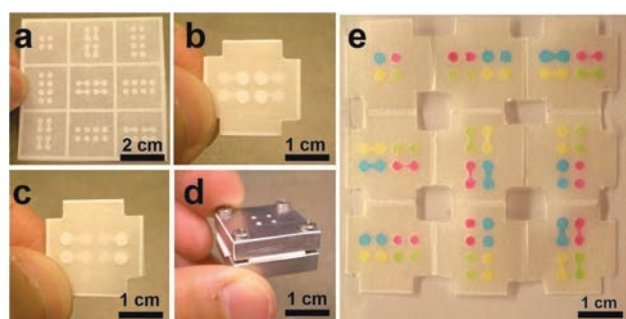


Figure 1. (a) Chromatography paper (100 μm thick) having photolithographically patterned channels, reservoirs, and a folding frame. All channels were 900 μm wide, and the reservoirs were 2.5 mm in diameter. (b) Top layer of the folded paper revealing four inlet reservoirs in the center of the device. The four flanking circular features are present within the 3-D structure of the device but are visible due to the transparency of the paper. Four corners of the folded paper were cut so it could be clamped in the aluminum housing shown in (d). (c) Bottom layer of the folded paper. (d) The aluminum housing used to support the 3-D paper microfluidic system. The four holes drilled in the top of the housing are used for injecting solutions. (e) An unfolded, nine-layer paper microfluidic device after injecting four 1.0 mM, aqueous, colored solutions (rhodamine 6G, red; eriochlorin, blue; tetracycline, yellow; and a mixture of eriochlorin and tetracycline, 1:10, green) through the four injection ports in the aluminum clamp. The colored solutions passed through their designated channels and reservoirs without mixing.

Importantly, this origami assembly method does not require adhesive tape, which can lead to contamination and nonspecific adsorption.³ Avoiding tape also speeds the assembly of the device and eliminates the need for laser cutting. The photoresist pattern serves as the channel wall to separate solutions into different channels in all three dimensions. As described previously,¹³ the vertical connections are made by direct contact of paper channels or reservoirs on adjacent layers, and this avoids the use of cellulose powders.³

The nine-layer device shown in Figure 1 was used to demonstrate the ability of the origami device to direct the flow of fluids in three dimensions. Specifically, 10.0 μL of the following four 1.0 mM aqueous solutions were injected through the openings in the top plate of the clamp: rhodamine 6G (red), eriochlorin (blue), tetracycline (yellow), and eriochlorin mixed with tetracycline (1:10, green). After 5 min, the device was unfolded, and, as shown in Figure 1e, the solutions flowed through their designated channels and reservoirs without mixing. Moreover, there was no observable nonspecific adsorption of dyes on the channel walls.

As mentioned earlier, every layer of the device can be used for parallel colorimetric analysis of multiple analytes. This is because the paper can be unfolded after analysis to reveal a permanent record of the assay. This aspect of the method might be useful for multiplexed detection and high-throughput screening. To demonstrate this principle, a two-analyte colorimetric assay of glucose and protein (bovine serum albumin, BSA) was carried out using a single 3-D *o*PAD device comprising five layers and assembled by origami. The experiment was performed as follows. First, the detection reservoirs (parts a and c of Figure 2) were preloaded with commercially available reagents for the colorimetric detection of glucose and BSA, and then the device, including the reagents, was dried at 20 $^{\circ}\text{C}$ for 30 min. The specific reactions leading to colorimetric detection are provided in the SI, Figure S2.

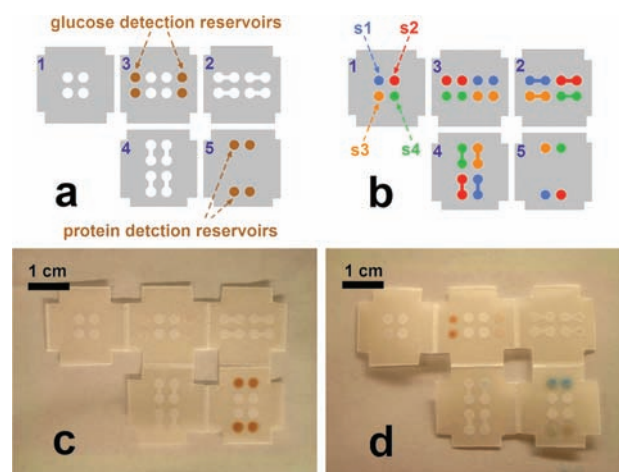


Figure 2. (a) Schematic diagram illustrating the design of the network used for assaying glucose and BSA. Note that the detection reservoirs for glucose and BSA are on different levels of the device. (b) Schematic diagram of the same network showing where the four samples were injected. Sample s1 was deionized water used as a control, sample s2 contained 5.6 mM glucose, sample s3 contained 4.5 μM BSA, and sample s4 contained 5.6 mM glucose plus 4.5 μM BSA. The numbers at the upper-left corner of the individual layers in (a) and (b) indicate the folding sequence for the device. (c) Photograph of an unfolded device showing the assay reagents dried in the detection reservoirs. (d) Unfolded 3-D device after completion of the assay. The color change from colorless to brown indicated the presence of glucose in samples s2 and s4. The color change from brown to blue indicated the presence of BSA in samples s3 and s4. No color change was observed for control sample s1.

Second, four 5.0 μL aliquots containing different amounts of glucose and BSA were injected into the four inlets at the top of the device (Figure 2b). The samples flowed toward the detection reservoirs, and a portion of these samples were allowed to react with the preloaded reagents for 10 min. Finally, the paper was unfolded so that both layers having detection reservoirs were accessible for colorimetric analysis. The degree of color change is directly related to the concentration of glucose or protein in the samples.

A comparison of parts c and d of Figure 2 indicates that the assay was successful and that there was no mixing between channels or reservoirs. Specifically, the color of the solution in the detection reservoirs exposed to glucose (samples s2 and s4, Figure 2b) or BSA (samples s3 and s4) changed from colorless to brown or from brown to blue, respectively. Although only two layers on the device were required for this very simple colorimetric assay, it is obvious that more complex analysis could be performed. To scale up the device for analyzing more analytes or more samples, additional layers might be required. However, since all layers of the multilayer network are fabricated simultaneously, the addition of more layers or more complex structures does not present much of a practical barrier.

Fluorescence detection usually provides substantially higher sensitivity and lower detection limits than simple colorimetric measurements. However, to the best of our knowledge, fluorescence detection has not thus far been used for 3-D *o*PAD-based assays. Accordingly, we fabricated three-layer *o*PADs (similar to the device illustrated in Figure 2b, but with just three layers) that could be used to carry out four simultaneous BSA assays using fluorescence detection. The assay is based on the dye epicoccone, which exhibits enhanced fluorescence in the presence

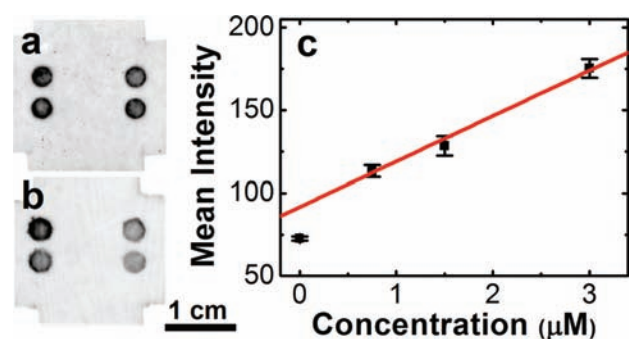


Figure 3. (a) and (b) Fluorescence images of the bottom layer of the unfolded oPAD revealing the four detection reservoirs. In (a) all four injected samples contained 3.00 μM BSA, while in (b) the BSA concentrations were 0 (bottom right), 0.75 μM (top right), 1.50 μM (bottom left), and 3.00 μM (top left), respectively. (c) Calibration curve for quantification of BSA. The mean fluorescence intensity was corrected for the background fluorescence of the paper. The error bars represent the standard deviation of at least three independent measurements. The data point corresponding to 0 BSA was not included in the fit (red line) as it is outside the linear detection range.

of BSA (Figure S3, SI).¹⁵ The assay for BSA using the paper device was carried out as follows. First, 1.0 μL of a buffered epicoccinone solution was spotted onto each detection reservoir and then dried at 20 $^{\circ}\text{C}$ for 5 min. Second, 3.0 μL aliquots of buffered BSA solutions were injected into the four inlets at the top of the device. Third, the oPAD was placed in a humidity chamber for 30 min, during which time the BSA solutions passed to the detection reservoirs and reacted with the preloaded fluorescent dye. Finally, the bottom layer of the device was scanned using a fluorescence imager. Each scan was performed at 100 μm resolution and was complete within 1 min.

Figure 3a shows the result of an assay in which all four BSA aliquots were of the same concentration (3.0 μM), while in Figure 3b the concentrations of BSA were different (0, 0.75, 1.50, and 3.00 μM). Qualitatively, Figure 3b shows that the color of the detection reservoirs becomes darker as the concentration of BSA increases. To quantify these results, the images were imported into Adobe Photoshop CS2 and transferred to gray-scale mode. The mean fluorescence intensity was determined from the image histogram for each detection reservoir, and then it was background-corrected by subtracting the average intensity measured at the center of the paper where no BSA was present. These data constitute a calibration curve, which is shown in Figure 3c. The error bars represent the standard deviation of at least three independent measurements. The detection limit, defined as 3 times the standard deviation of the sample containing no BSA (0 μM) divided by the slope of the calibration curve, is 0.14 μM BSA. Because the fluorescence intensity, rather than the color change, is directly proportional to protein concentration, quantification by fluorescence is more straightforward than colorimetric detection.

To summarize, we have reported an origami-based method for fabricating 3-D paper microfluidic devices. This method provides a number of key advantages compared to previously reported approaches that rely on stacking individual layers and holding them in place with double-sided tape. First, origami fabrication only requires one photolithographic patterning step, regardless of the number of layers. Therefore, the devices can be made arbitrarily complex without much additional fabrication overhead. Second, oPADs can be produced by automated printing techniques and

subsequently assembled without tools. Third, detection points can be placed on any layer of oPADs, because the paper can be easily unfolded to reveal them. Fourth, the resulting permanent record of an assay can be qualitatively analyzed using the naked eye, or the results can be quantified using a high-throughput automated scanner. We believe oPADs will prove promising for applications that involve low cost and simplicity.

■ ASSOCIATED CONTENT

S Supporting Information. Information about chemicals, materials, experimental procedures, and the assay reactions. This material is available free of charge via the Internet at <http://pubs.acs.org>.

■ AUTHOR INFORMATION

Corresponding Author
crooks@cm.utexas.edu

■ ACKNOWLEDGMENT

We gratefully acknowledge support from the Chemical Sciences, Geosciences, and Biosciences Division, Office of Basic Energy Sciences, Office of Science, U.S. Department of Energy (Contract No. DE-FG02-06ER15758). We also thank the U.S. Army Research Office (Grant No. W911NF-07-1-0330) and the U.S. Defense Threat Reduction Agency for financial support. The Robert A. Welch Foundation provides sustained support for our research (Grant F-0032). We thank Cecil Harkey of the UT-Austin ICMB for help with the fluorescence imager and Jim Loussaert for help with the fluorimeter measurements.

■ REFERENCES

- (1) Unger, M. A.; Chou, H. P.; Thorsen, T.; Scherer, A.; Quake, S. R. *Science* **2000**, *288*, 113–116.
- (2) Kartalov, E. P.; Walker, C.; Taylor, C. R.; Anderson, W. F.; Scherer, A. *Proc. Natl. Acad. Sci. U.S.A.* **2006**, *103*, 12280–12284.
- (3) Martinez, A. W.; Phillips, S. T.; Whitesides, G. M. *Proc. Natl. Acad. Sci. U.S.A.* **2008**, *105*, 19606–19611.
- (4) Martinez, A. W.; Phillips, S. T.; Butte, M. J.; Whitesides, G. M. *Angew. Chem., Int. Ed.* **2007**, *46*, 1318–1320.
- (5) Martinez, A. W.; Phillips, S. T.; Wiley, B. J.; Gupta, M.; Whitesides, G. M. *Lab Chip* **2008**, *8*, 2146–2150.
- (6) Cheng, C. M.; Martinez, A. W.; Gong, J. L.; Mace, C. R.; Phillips, S. T.; Carrilho, E.; Mirica, K. A.; Whitesides, G. M. *Angew. Chem., Int. Ed.* **2010**, *49*, 4771–4774.
- (7) Nie, Z. H.; Nijhuis, C. A.; Gong, J. L.; Chen, X.; Kumachev, A.; Martinez, A. W.; Narovlyansky, M.; Whitesides, G. M. *Lab Chip* **2010**, *10*, 477–483.
- (8) Dungchai, W.; Chailapakul, O.; Henry, C. S. *Anal. Chem.* **2009**, *81*, 5821–5826.
- (9) Lu, Y.; Shi, W. W.; Jiang, L.; Qin, J. H.; Lin, B. C. *Electrophoresis* **2009**, *30*, 1497–1500.
- (10) Osborn, J. L.; Lutz, B.; Fu, E.; Kauffman, P.; Stevens, D. Y.; Yager, P. *Lab Chip* **2010**, *10*, 2659–2665.
- (11) Nie, Z. H.; Deiss, F.; Liu, X. Y.; Akbulut, O.; Whitesides, G. M. *Lab Chip* **2010**, *10*, 3163–3169.
- (12) Martinez, A. W.; Phillips, S. T.; Whitesides, G. M.; Carrilho, E. *Anal. Chem.* **2010**, *82*, 3–10.
- (13) Martinez, A. W.; Phillips, S. T.; Nie, Z. H.; Cheng, C. M.; Carrilho, E.; Wiley, B. J.; Whitesides, G. M. *Lab Chip* **2010**, *10*, 2499–2504.
- (14) Siegel, A. C.; Phillips, S. T.; Dickey, M. D.; Lu, N. S.; Suo, Z. G.; Whitesides, G. M. *Adv. Funct. Mater.* **2010**, *20*, 28–35.
- (15) Bell, P. J. L.; Karuso, P. *J. Am. Chem. Soc.* **2003**, *125*, 9304–9305.